



# Independent Relationship between Amyloid Precursor Protein (APP) Dimerization and $\gamma$ -Secretase Processivity

Joo In Jung<sup>1,2,3</sup>, Sasha Premraj<sup>1,4</sup>, Pedro E. Cruz<sup>1,2,3</sup>, Thomas B. Ladd<sup>1,2,3</sup>, Yewon Kwak<sup>1</sup>, Edward H. Koo<sup>5</sup>, Kevin M. Felsenstein<sup>1,2,3</sup>, Todd E. Golde<sup>1,2,3\*</sup>, Yong Ran<sup>1,2,3\*</sup>

**1** Center for Translational Research in Neurodegenerative Disease, University of Florida, Gainesville, Florida, United States of America, **2** Department of Neuroscience, University of Florida, Gainesville, Florida, United States of America, **3** McKnight Brain Institute, College of Medicine, University of Florida, Gainesville, Florida, United States of America, **4** College of Pharmacy, University of Florida, Gainesville, Florida, United States of America, **5** Department of Neuroscience, University of California San Diego, La Jolla, California, United States of America

## Abstract

Altered production of  $\beta$ -amyloid ( $A\beta$ ) from the amyloid precursor protein (APP) is closely associated with Alzheimer's disease (AD). APP has a number of homo- and hetero-dimerizing domains, and studies have suggested that dimerization of  $\beta$ -secretase derived APP carboxyl terminal fragment (CTF $\beta$ , C99) impairs processive cleavage by  $\gamma$ -secretase increasing production of long  $A\beta$ s (e.g.,  $A\beta$ 1-42, 43). Other studies report that APP CTF $\beta$  dimers are not  $\gamma$ -secretase substrates. We revisited this issue due to observations made with an artificial APP mutant referred to as 3xK-APP, which contains three lysine residues at the border of the APP ectodomain and transmembrane domain (TMD). This mutant, which dramatically increases production of long  $A\beta$ , was found to form SDS-stable APP dimers, once again suggesting a mechanistic link between dimerization and increased production of long  $A\beta$ . To further evaluate how multimerization of substrate affects both initial  $\gamma$ -secretase cleavage and subsequent processivity, we generated recombinant wild type- (WT) and 3xK-C100 substrates, isolated monomeric, dimeric and trimeric forms of these proteins, and evaluated both  $\epsilon$ -cleavage site utilization and  $A\beta$  production. These show that multimerization significantly impedes  $\gamma$ -secretase cleavage, irrespective of substrate sequence. Further, the monomeric form of the 3xK-C100 mutant increased long  $A\beta$  production without altering the initial  $\epsilon$ -cleavage utilization. These data confirm and extend previous studies showing that dimeric substrates are not efficient  $\gamma$ -secretase substrates, and demonstrate that primary sequence determinants within APP substrate alter  $\gamma$ -secretase processivity.

**Citation:** Jung JI, Premraj S, Cruz PE, Ladd TB, Kwak Y, et al. (2014) Independent Relationship between Amyloid Precursor Protein (APP) Dimerization and  $\gamma$ -Secretase Processivity. PLoS ONE 9(10): e111553. doi:10.1371/journal.pone.0111553

**Editor:** Jaya Padmanabhan, University of S. Florida College of Medicine, United States of America

**Received:** July 15, 2014; **Accepted:** September 28, 2014; **Published:** October 28, 2014

**Copyright:** © 2014 Jung et al. This is an open-access article distributed under the terms of the Creative Commons Attribution License, which permits unrestricted use, distribution, and reproduction in any medium, provided the original author and source are credited.

**Data Availability:** The authors confirm that all data underlying the findings are fully available without restriction. All relevant data are within the paper and its Supporting Information files.

**Funding:** This work was supported by National Institutes of Health (NIH) Grant AG202063 to TG. The funders had no role in study design, data collection and analysis, decision to publish, or preparation of the manuscript.

**Competing Interests:** The authors have declared that no competing interests exist.

\* Email: tgolde@mbi.ufl.edu (TEG); yran@ufl.edu (YR)

## Introduction

The amyloid  $\beta$  ( $A\beta$ ) peptide is the core component of senile plaques in Alzheimer's disease (AD) brains [1,2,3]. This peptide is produced from the amyloid precursor protein (APP) by sequential cleavages of  $\beta$ -secretase and  $\gamma$ -secretase [4].  $\beta$ -Secretase cleavage releases the ectodomain of APP and produces the 99 amino acid membrane-anchored CTF $\beta$ . CTF $\beta$  is subsequently cleaved by  $\gamma$ -secretase to produce various  $A\beta$  isoforms and APP intracellular domain (AICD) fragments [5].  $A\beta$  has multiple isoforms [6,7].  $A\beta$ 40 is typically the major species produced, whereas  $A\beta$ 37,  $A\beta$ 38,  $A\beta$ 39, and  $A\beta$ 42 are produced at lower levels. Other  $A\beta$  isoforms including  $A\beta$ 34,  $A\beta$ 41, and  $A\beta$ 43 are produced under various circumstances [6,8,9,10]. Relative increases in long  $A\beta$ s (i.e.,  $A\beta$ 42 or  $A\beta$ 43) are tightly linked to increased risk for AD and biologically related to the increased propensity for these long  $A\beta$ s to aggregate [11]. Many presenilin (*PSEN*) and *APP* mutations linked to early onset familial AD (FAD) increase the relative amount of  $A\beta$ 42/ $A\beta$ 40 in *in vitro* and *in vivo* paradigms [12,13,14,15].  $A\beta$ x-42 has been shown to be the earliest form of

$A\beta$  in AD brains [16,17,18].  $A\beta$ 42 has a much stronger tendency to aggregate than  $A\beta$ 40 [19,20]. In addition,  $A\beta$ 42 seeding is essential for parenchymal and vascular amyloid deposition in mice [21].  $A\beta$ 43 has similar aggregation properties both *in vitro* and *in vivo* [22,23].

Elegant studies from Ihara and colleagues that have now been confirmed and extended demonstrate that  $\gamma$ -secretase cleavage of APP occurs initially at  $\epsilon$ -sites near the cytoplasmic face of the TMD in CTF $\beta$ . Subsequently, variable numbers of step-wise carboxyl peptidase-like cleavages of 3–5+ amino acids combined with different initial  $\epsilon$ -cleavage site utilization produce the various levels of the different  $A\beta$  peptides [10,24,25]. Increased long  $A\beta$  can thus arise from altered  $\epsilon$ -cleavage site utilization, decreased step-wise cleavage (processivity), or a combination of these two. Multhaup and colleagues have proposed that when CTF $\beta$  forms dimers,  $\gamma$ -secretase processivity is reduced due to steric hindrance by interhelical interactions of the tandem TMD GXXXG motifs, leading to increased long  $A\beta$  isoforms [26,27]. Specifically, they reported that artificial mutations that induce CTF $\beta$  dimerization

increase long A $\beta$  or, alternatively, alterations in the GXXXG motif that inhibit dimerization decreased long A $\beta$  along with increase in short A $\beta$ s. Further, they linked this effect on dimerization to mechanisms of action of NSAID based acidic  $\gamma$ -secretase modulators (GSMs) that decrease long A $\beta$  production by increasing  $\gamma$ -secretase processivity [28]. The binding site for GSM can be shown to overlap with the GXXXG motif in APP [28,29]; they decrease production of long A $\beta$  by promoting processivity and have been shown to reduce dimerization of APP. In some cases, small molecules that inhibit APP homodimerization reduce A $\beta$ 40 production along with long A $\beta$ 42 although their effects appear to additionally involve inhibition of  $\beta$ -secretase activity [30]. Despite these interesting data that associate dimerization of substrate with increased long A $\beta$  production, multiple studies have not seen this association reporting that dimerization decreases or even blocks substrate cleavage by  $\gamma$ -secretase. An APP protein with a FK506-binding protein (FKBP) fused to the C-terminus of APP could be cleaved normally by  $\gamma$ -secretase [31], however, following addition of the synthetic membrane-permeable drug AP20187, which induced dimerization of the APP-FKBP chimera, showed markedly decreased total A $\beta$  levels due to inhibited  $\gamma$ -cleavage [31]. Dimerization of other  $\gamma$ -secretase substrates such as Notch or Glycophorin A has also been shown to reduce  $\gamma$ -secretase cleavage studied in *Drosophila* [32,33,34].

Although we felt the weight of the evidence suggested that APP dimerization reduces or prevents  $\gamma$ -secretase cleavage, an unexpected finding was provocative enough that we decided to revisit this issue. We have recently reported that an artificial APP mutant (referred to as 3xK-APP or G29K/A30K) with three lysines immediately downstream of the juxtamembrane domain (JMD) (See Figure 1A) dramatically increases both A $\beta$ 42 and A $\beta$ 43 by decreasing  $\gamma$ -secretase processivity [9]. In subsequent studies reported here, we have found that the 3xK-APP formed SDS-stable dimers. Thus, it seemed plausible that the 3xK-APP increased substrate dimerization and this increased the long A $\beta$  isoforms. To directly evaluate the relationship between dimerization and A $\beta$  production, we produced the APP-based substrates, recombinant WT-C100Flag and 3xK-C100Flag substrates, and took advantage of the fact that these substrates form SDS-stable multimers that can be resolved on and purified from SDS-PAGE gels [35]. Monomers, dimers, and trimers of the two recombinant substrates could be isolated and were shown to remain predominantly in their initially purified form after  $\gamma$ -secretase activity assays, indicating little major alterations in aggregation state following the activity assay. Using both ELISA and immunoprecipitation-mass spectrometry (IP/MS) to assess cleavage of these substrates in *in vitro*  $\gamma$ -secretase cleavage assays, we find i) that the dimers and trimers of WT and 3xK substrates are not cleaved efficiently by  $\gamma$ -secretase cleavage and ii) that increased levels of the long A $\beta$  peptides are produced from monomeric 3xK substrate without alterations in  $\epsilon$ -site utilization. These studies indicate that alterations in  $\gamma$ -secretase processivity are not attributable to dimerization of substrate, but, rather, dependent on primary sequence of the substrate.

## Materials and Methods

### Cell culture

Chinese hamster ovary cells (CHO) stably overexpressing APP695wt and G29K/A30K(3xK)-APP695wt [9] were grown in Ham's F-12 medium (Life Technologies) supplemented with 10% fetal bovine serum and 100 units/ml of penicillin and 100  $\mu$ g/ml streptomycin. Cells were grown at 37°C in a humidified atmosphere containing 5% CO<sub>2</sub> in tissue culture plates (Costar).

The cells were harvested at confluence, and then utilized for biochemical analyses.

### Western Blotting

Each of the WT-APP and the 3xK-APP expressing cells were harvested and lysed in radioimmunoprecipitation assay (RIPA) buffer (Tris-HCl, pH 7.4 50 mM, NaCl 150 mM, Triton X100 1%, Sodium deoxycholate 0.5%, SDS 0.1%) [36]. For APP dimer/monomer detection, we utilized 3–8% Tris-Acetate gels (Biorad) and for CTF detection we used 10% Bis-Tris gels (Biorad). The lysates were subsequently used for immunoblotting and detection of full-length APP and carboxyl terminal fragments (CTFs). APP C-terminal specific polyclonal antibody A8717 (1:500) (Sigma-Aldrich) was used for the APP and CTF $\alpha$ / $\beta$  detection. For recombinant substrate detection, we used 4–12% Bis-Tris gels (Biorad) and detected with monoclonal 6E10 antibody (1:1000) (Covance, Emeryville, CA, USA). The blots were developed using an Odyssey infrared scanner (LiCor Biosciences, Lincoln, NE, USA).

### Mass Spectrometry of A $\beta$

Conditioned media from WT-APP and 3xK-APP cells were harvested and used to analyze secreted A $\beta$  profiles using matrix-assisted laser desorption/ionization time of flight (MALDI-TOF) mass spectrometry analysis. Secreted A $\beta$  peptides from conditioned media were analyzed as previously described with the following modifications [37,38,39]. Briefly, the A $\beta$  peptides were immunoprecipitated using Ab5 recognizing the A $\beta$ 1-16 epitope [40] and sheep anti-mouse IgG magnetic Dynabeads (Life Technologies, catalog no. 11201D) and eluted with 0.1% trifluoroacetic acid (TFA) in water. Eluted samples were mixed 2:1 with saturated  $\alpha$ -cyano-4-hydroxycinnamic acid (CHCA) matrix (Sigma) in mixture of acetonitrile (60%) and methanol (40%) and loaded onto a CHCA pretreated MSP 96 target plate-polished steel (Bruker, Billerica, MA, USA - Part No. 224989). Samples were analyzed using a Bruker Microflex LRF-MALDI-TOF mass spectrometer. The theoretical average molecular weights of A $\beta$  and AICD fragments were calculated using Expasy Compute pI/Mw tool.

### A $\beta$ ELISAs

Monoclonal antibodies to A $\beta$  were generated by the Mayo Clinic Immunology Core facilities (Jacksonville, FL, USA). Ab13.1.1. was raised against A $\beta$ 35-40 and is specific for A $\beta$ x-40, and exhibits minimal cross-reactivity with other A $\beta$  peptides. Ab 2.1.3 was raised against A $\beta$ 35-42 and is specific for A $\beta$ x-42. The A $\beta$ 38 antibody (Ab38), supplied by P. Mehta (Institute of Basic Research, Staten Island, NY, USA), specifically recognizes A $\beta$ x-38 and shows no cross-reactivity with other A $\beta$  peptides. For cell-based screens, A $\beta$  was captured from conditioned medium with either Ab5, Ab38, Ab13.1.1, or Ab2.1.3 (coated at 10–50  $\mu$ g/ml in EC buffer: 5 mM NaH<sub>2</sub>PO<sub>4</sub>-H<sub>2</sub>O, 20 mM Na<sub>2</sub>HPO<sub>4</sub>, 400 mM NaCl, 2.5 mM EDTA, 150  $\mu$ M BSA, 800  $\mu$ M CHAPS, and 8 mM NaN<sub>3</sub>) on Immulon 4HBX Flat-Bottom Microfilter 96-well plates (Thermo Scientific, Waltham, MA, USA). A $\beta$  peptides were detected with HRP-conjugated Ab5 (epitope in the amino terminus of A $\beta$ 1-16). A $\beta$  standards (Bachem, King of Prussia, PA, USA) were prepared by dissolving in hexafluoroisopropanol (HFIP) at 1 mg/ml with sonication, dried under nitrogen, resuspended at 2 mg/ml HFIP, sonicated again and dried under nitrogen. The resulting A $\beta$  was resuspended in 0.01% ammonium hydroxide, portioned into aliquots in EC buffer, and frozen at –80°C. Following these steps, the A $\beta$  is monomeric, as determined by size-exclusion chromatography.

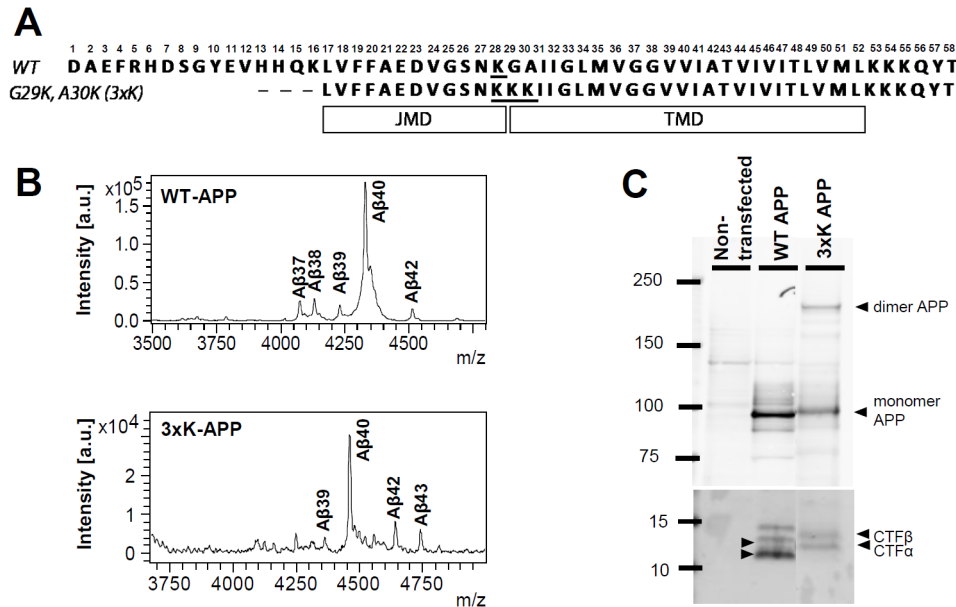


**Figure 1. An APP dimer in 3xK-APP mutant-overexpressing CHO cells.** (A) Schematic of WT-APP and 3xK-APP mutant. (B) A $\beta$  profile analyzed by IP/MS demonstrated increased A $\beta$ 42 and A $\beta$ 43 levels of the mutant compared to WT. (C) APP dimer bands migrated at  $\sim$ 200 kDa along with APP monomer bands at  $\sim$ 100 kDa in a 3–8% tris-acetate gel. Both WT APP and 3xK-APP were normally processed to CTF $\alpha$  and CTF $\beta$ , but 3xK-APP produced less CTF $\alpha$  and CTF $\beta$  than WT-APP (Also see Figure S1 in File S1). doi:10.1371/journal.pone.0111553.g001

### Recombinant Protein Production and Extraction

Recombinant DNAs encoding WT-C100Flag [35,41] or 3xK-C100Flag [9] were produced and cloned into pET-21b+ vectors (Life Technologies). The proteins were overexpressed and purified from *Escherichia coli* BL21 using HiTrap Q-column (GE Life Science, Little Chalfont, UK). The recombinant proteins were mixed with sample buffer and run on the precast 4–12% Bis-Tris gels (BioRad) for western blotting to determine the size of monomer, dimer, and trimer forms of the proteins. N-terminal specific antibody 6E10 (Covance, Gaithersburg, MD) was used to detect the oligomers of the recombinant proteins. After the size is determined, the monomer, dimer, and trimer of each protein are directly excised from the preparative gels that were loaded with our protein samples. Each of the excised gel parts was pestled in 150 mM Sodium Citrate buffer (pH 6.8). The supernatant containing the elute is used for further validation of oligomeric state by rerunning them on 4–12% Bis-Tris gels and stained using Coomassie blue solution and immunoblotted with Ab5 antibody. The concentration of monomer, dimer, and trimer was determined using BCA assays (Thermo Scientific). The eluates were further utilized for *in vitro*  $\gamma$ -secretase assay.

### *In vitro* $\gamma$ -secretase assay

For the *in vitro*  $\gamma$ -secretase assay, 25  $\mu$ g/mL of each substrate was incubated with the membrane containing  $\gamma$ -secretase [42] (100  $\mu$ g/ml total proteins) in 150 mM sodium citrate buffer, pH 6.8, containing complete protease inhibitor (Roche, Indianapolis, IN, USA) for 2 hours at 37°C. The A $\beta$  peptides were captured using Ab5 bound to sheep anti-mouse IgG magnetic Dynabeads. The AICD fragments were captured using anti-FLAG M2 magnetic beads (Sigma). Anti-FLAG M2 magnetic beads are anti-FLAG M2 (mouse monoclonal) antibody attached to superparamagnetic iron and then bound to 4% agarose beads. The M2 antibody recognizes FLAG sequence (DYKDDDDK) at the N-terminus, (Met-N-terminus) and C-terminus. The beads were then

washed with water and the fragments eluted using 0.1% TFA (Thermo Scientific) in water. The eluted fragments were further processed for MS, as described above.

### Statistical analysis

*In vitro* data were expressed and graphed as the mean  $\pm$  SEM using GraphPad Prism 5 software. Analysis was by two-way analysis of variance (ANOVA) followed by bonferroni post-hoc testing for group differences. The level of significance was set at  $p < 0.05$  in all tests.

## Results

### 3xK-APP Mutant Dimerization in CHO Cells

In our previous studies examining the interaction between substrate sequence and GSM activity, we have found that an artificial APP mutant (referred to as 3xK-APP) with three lysines immediately downstream of the JMD in APP dramatically increases both A $\beta$ 42 and A $\beta$ 43 by decreasing  $\gamma$ -secretase processivity [9]. Figure 1A shows JMD-TMD sequences of WT-APP and 3xK-APP CTF $\beta$ , and representative A $\beta$  profiles from IP/MS study of WT-APP and 3xK-APP are shown in Figure 1B. Subsequently, Western blot analysis of the 3xK APP extracted from a stable CHO cell line revealed the expected APP monomeric holoprotein migrating at molecular weight  $\sim$ 100– $\sim$ 120 kDa, as well as a species consistent with a holoprotein dimer migrating at  $\sim$ 200+ kDa weight (Figure 1C). This 200+ kDa APP species was not observed in a CHO cell line overexpressing WT APP. As previously reported, 3xK-APP was processed into CTF $\alpha$  and CTF $\beta$ ; though both bands migrate slower on SDS-PAGE than the WT CTFs (Figure 1C). The Western blot in Figure 1C was probed with anti-APP C-terminal antibody (A8717) that detects both CTF $\alpha$  and CTF $\beta$ . Furthermore, we explicitly indicate CTF $\beta$  expression for WT-APP and 3xK-APP by using two A $\beta$  N-terminal specific antibodies, 6E10 and 82E1 (Figure S1 in File S1). Consistent with the observation in CTF $\beta$  detected with A8717

antibody (Figure 1C), 3xK-CTF $\beta$  bands probed with 6E10 and 82E1 antibodies showed slower migration on SDS-PAGE than the WT-CTF $\beta$  (Figure S1 in File S1).

### Dimers and Trimers of Recombinant APP substrate Decrease A $\beta$ Production

Given conflicting data in the literature as to whether a dimeric substrate could be cleaved by  $\gamma$ -secretase and account for shifts in processivity of  $\gamma$ -secretase towards longer A $\beta$  peptides, we directly tested if decreased  $\gamma$ -secretase processivity resulting from long A $\beta$  production is influenced by substrate dimer or trimer formation using an *in vitro* system. Recombinant WT-C100Flag that serves as an APP substrate akin to CTF $\beta$  was used for  $\gamma$ -secretase cleavage assay after additional extraction steps for obtaining its monomer, dimer, and trimer forms. One notable characteristic of this recombinant substrate is the ability to aggregate rapidly and form SDS stable multimers that can be resolved by SDS-PAGE (Figure S2A in File S1) [35]. Figure S2A in File S1 illustrates WT-C100Flag monomer and multimer substrates analyzed by Western blot using a CTF $\beta$  detecting antibody (6E10) after SDS-PAGE. Following a preparative SDS-PAGE, we purified WT-C100Flag monomers, dimers, and trimers by directly cutting and eluting the bands from the gel at  $\sim 12$  kDa (monomers),  $\sim 24$  kDa (dimers), and  $\sim 36$  kDa (trimers) (Figure 2A). The concentrations of the eluates measured from monomer, dimer, and trimer substrates were 1.6 mg/mL, 1.8 mg/mL, and 0.9 mg/mL, respectively. Following elution from the gel, purity and stability were then assessed by running the purified proteins on SDS-PAGE and Western blotting following purification and after incubation in an *in vitro*  $\gamma$ -secretase cleavage assay (IVA) (Figure 2B, 2C). The eluates were used at 25  $\mu$ g/mL for IVA. When initially purified the monomer remains as monomer, the dimer partially dissociates into monomer and aggregates further; the purified trimer also aggregates further and dissociates into dimer and monomer. This pattern was also observed following the IVA; with the exception that monomer forms a small amount of dimer. Following the IVA, from each group, A $\beta$  levels were measured by specific A $\beta$  ELISAs (Figure 2D), and A $\beta$  and AICD profiles were analyzed by IP/MS (Figure 2E and 2F). As assessed by ELISA, A $\beta$  production was significantly decreased when WT-C100Flag dimers and trimers were used as substrates. Notably, purified monomer was a much more efficient substrate than non-purified substrate. In multiple assays, the purified substrate was cleaved  $\sim 10$ – $\sim 14$  times more efficiently. Further, IP/MS and ELISA showed no evidence for alterations in A $\beta$  profiles; all species diminished equally (Figure 2D and 2E). Similarly, when assessed by IP/MS there was no major shift in  $\epsilon$ -site utilization (Figure 2F). Although our results could be confounded by challenges in detecting aggregates of the cleavage products, we do not think that this is the case. The ELISAs employed efficiently recognize various A $\beta$  aggregate assemblies [18]. Thus, it is unlikely that dimeric or trimeric substrates are generating dimeric or trimeric cleavage products that are escaping detection. As to whether the A $\beta$  generated from the dimeric substrate remains dimeric is challenging to address as the solvents used for IP/MS studies could dissociate a dimer into monomers. This would also be challenging to address by gel-based methods given the large amounts of substrate used and the potential for artifactual dimerization of A $\beta$  [43]. As the purified dimer appears capable of dissociating into monomer, the simplest explanation for this observation is that  $\gamma$ -secretase cleaves monomer substrate following dissociation of the dimer.

### Effect of 3K-C100Flag on A $\beta$ 42 production is independent of its dimerization

Given these findings, we tested whether 3xK-APP substrate can increase long A $\beta$  peptides without dimerization. As with non-purified WT-C100Flag substrate (Figure S2A in File S1), non-purified 3xK-C100Flag substrate rapidly aggregated and formed SDS-stable multimers on SDS-PAGE gels. 3xK-C100Flag substrate monomers and multimers were further detected by Western blot (Figure S2B in File S1). Using methods described above, monomer, dimer and trimer of 3xK-C100Flag were purified and analyzed after purification and IVA (Figure 3A–3C). The concentrations of the 3xK-C100Flag eluates measured from monomer, dimer, and trimer substrates were 0.95 mg/mL, 0.9 mg/mL, and 1.2 mg/mL, respectively. As for 3xK-C100Flag, 25  $\mu$ g/mL of each eluate was utilized for the IVAs. Analysis of A $\beta$  production and  $\epsilon$ -cleavage site showed that as observed with the WT substrate, multimerization of the mutant substrate impedes  $\gamma$ -secretase cleavage. A $\beta$  levels measured from 3xK-C100Flag dimer and trimer were significantly less than its monomer when analyzed by A $\beta$  specific ELISAs (Figure 3D). This was further confirmed by A $\beta$  and AICD profiles illustrated from IP/MS. 3xK-C100Flag monomer increased the relative production of long A $\beta$  species, A $\beta$ 42 and A $\beta$ 45, without significantly altering  $\epsilon$ -site utilization (Figure 3E, 3F). Notably, the mutant monomer showed no evidence for aggregation after the IVA (Figure 3C). As discussed for the WT-C100Flag substrate, the A $\beta$  produced from the 3xK-C100Flag dimer substrate could arise from  $\gamma$ -secretase cleavage of 3xK-C100Flag dimers or dissociating 3xK-C100Flag monomers.

### Discussion

Previous studies have yielded conflicting results regarding the effects of substrate dimerization on  $\gamma$ -secretase cleavage of APP. Here we have revisited this issue with purified recombinant monomeric, dimeric, and trimeric substrates. Under conditions in which monomeric substrate is cleaved efficiently by  $\gamma$ -secretase *in vitro*, the dimeric and trimeric substrates are cleaved very inefficiently. Following purification of the dimeric and trimeric substrates, we present evidence that these assemblies can, to some degree, dissociate into monomer based on their non-covalent interactions; thus, we attribute the minor amount of  $\gamma$ -secretase cleavage of the dimer and trimer not to cleavage of dimer or trimer but to cleavage of monomer following disassociation; however, we cannot completely exclude the possibility that multimers are cleaved by  $\gamma$ -secretase with decreased efficiency. Further, we find no evidence that APP substrate dimers, even if they were cleaved by  $\gamma$ -secretase, alter  $\gamma$ -secretase processivity. The profiles of A $\beta$  peptides generated during of the IVA of a dimeric substrate are not different from monomer. We show that effects of the 3xK-APP mutant substrate that does decrease  $\gamma$ -secretase processivity are observed when the substrate is monomeric. Thus, although this mutant promotes apparent dimerization of APP and increases long A $\beta$  production in cells, the effects of the mutation on APP dimerization and increase in long A $\beta$  appear mechanistically unrelated.

We chose to use an *in vitro* system where we could better control and monitor the aggregation state of the input substrate. We used a gel-purification method that generated well-characterized recombinant monomer and multimer substrates for  $\gamma$ -secretase activity assays. Although we did not rigorously attempt to address structure of our substrates, there is evidence that  $\alpha$ -helical conformation of the substrate critical for its dimerization is well preserved in the presence of SDS [35,44]. Further we find that gel-purified C100Flag monomer is much more efficiently

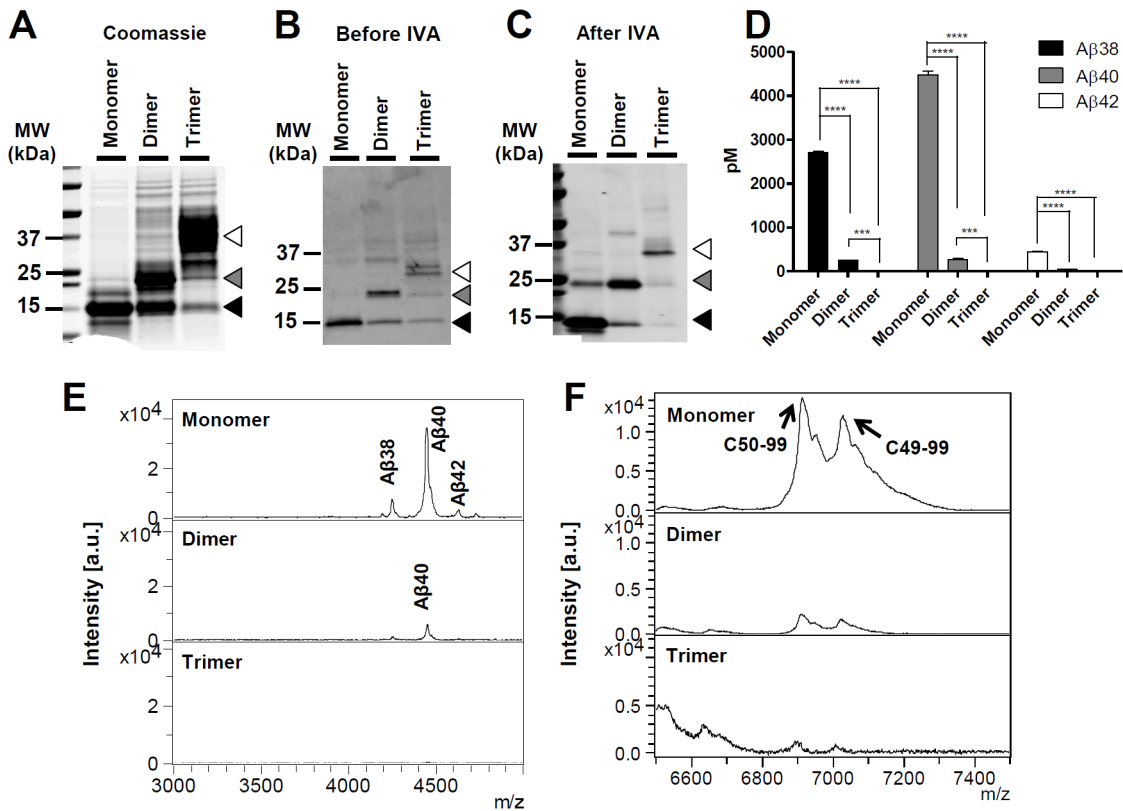


**Figure 2. Purified recombinant WT-C100Flag dimer and trimer showed reduced A $\beta$  production.** (A) The purified recombinant WT-C100Flag monomer, dimer, and trimer eluates were loaded on a SDS-PAGE gel. WT-C100Flag formed into SDS-stable monomer, dimer, and trimer shown by Coomassie staining. Monomer band was identified at  $\sim$ 12 kDa (closed arrow), dimer band was identified at  $\sim$ 24 kDa (grey arrow), and trimer band was at  $\sim$ 36 kDa (open arrow). (B) Monomer, dimer, and trimer WT-C100Flag extracted from a preparative gel were evaluated by Western blotting with 6E10 antibody before and after IVA. For IVA, the equal concentration of monomer, dimer, and trimer substrate was utilized (25  $\mu$ g/mL). (C) The purified substrates maintained largely remain as monomer, dimer or trimer following IVA, with an exception that a small amount of monomer aggregated into dimer. (D) The concentrations of A $\beta$  peptides generated during an *in vitro*  $\gamma$ -secretase assay were measured using sandwich ELISAs. A $\beta$ 38, A $\beta$ 40 and A $\beta$ 42 levels decreased in dimer compared to monomer, and the A $\beta$  levels for trimer were under detection limits. (E) A $\beta$  and (F) AICD profiles of C100Flag monomer, dimer, and trimer are characterized using IP/MS analyses. For identification of A $\beta$  species and AICD fragments, the calculated mass is compared with the observed mass, italicized in parentheses: For monomeric substrate, A $\beta$ 38 is 4261.064 (4262.78), A $\beta$ 40 is 4457.945 (4461.05), A $\beta$ 42 is 4640.108 (4645.29), and AICD50-99 is 6916.021 (6905.66), AICD49-99 is 7028.590 (7018.82). For the dimeric substrate, A $\beta$ 40 is 4459.094 (4461.05) and AICD50-99 is 6913.934 (6905.66) and AICD49-99 is 7026.387 (7018.82). This experiment was repeated 3 times with 2–3 replicates each time. Results were analyzed by two way analysis of variance (ANOVA) followed by bonferroni post hoc testing (\*\*\*\* $p$ <0.0001, \*\*\* $p$ <0.001).

doi:10.1371/journal.pone.0111553.g002

cleaved than non-gel purified substrate. Our studies are consistent with studies using mammalian cell based or *Drosophila* systems that have previously shown that  $\gamma$ -secretase does not cleave substrate dimers or at least does not cleave them efficiently [32,34]. Thus, these previous findings and our current findings are collectively inconsistent with the hypothesis that dimerization simply decreases  $\gamma$ -secretase processivity. Even the most direct data supporting the relationship between APP substrate dimerization and increased A $\beta$ 42 production (i.e., inducing disulfide linkage with K28C mutation) [27] could not be independently confirmed [31]. Hence, the changes in A $\beta$  peptides reported by Multhaup and colleagues may be attributable to the effects of the cysteine mutation on processivity of the monomeric substrate [27], rather than a consequence of dimerization. The effect of dimerization was also linked to the mechanism of action for NSAID-based GSMs and iGSMs. It is an appealing hypothesis that some GSMs that can bind at or near the tandem GXXXXG motifs [28,29] in APP can modulate cleavage by inhibiting dimer formation [28]; however, given our studies showing that amino acid sequence of monomeric substrate determines  $\gamma$ -secretase

processivity, GSMs likely modulate the property of the monomeric substrate to enhance  $\gamma$ -secretase processivity. Further, if the homodimerization competes with GSM binding, it is difficult to explain the allosteric models of GSM activity through GSM's  $\gamma$ -secretase complex binding [45,46,47,48,49] or possible tripartite interactions between  $\gamma$ -secretase, CTF $\beta$ -APP, and GSMs [9].

Although these and other data show that APP substrate dimerization is dissociable from effects on  $\gamma$ -secretase processivity, there remains an intriguing parallel between factors that alter dimerization and factors that alter  $\gamma$ -secretase processivity. Given the tandem GXXXXG motif functions as a glycine zipper to induce dimer formation not only in APP but in other proteins as well, we speculate that mutations like the 3xK-APP may i) anchor the TMD more rigidly within the membrane promoting alignment of the glycine zipper and favoring dimerization or ii) by removing the first of three glycine residues in the zipper promote alignment [50,51]. It is an intriguing possibility that 3xK-APP holoprotein dimerization could be attributable to disruption of cholesterol binding within the tandem GXXXXG motifs [52]; however, our data shows this effect on the holoprotein is likely not related to



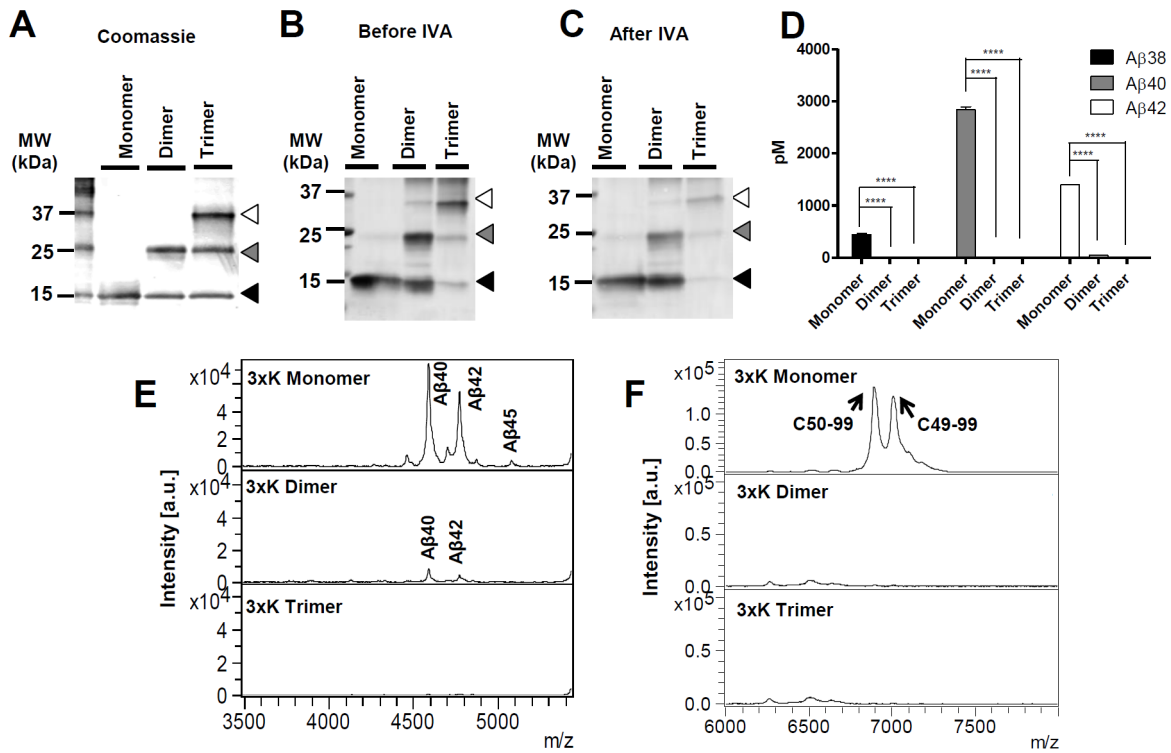


**Figure 3. Recombinant 3xK-C100Flag monomer increased longer Aβ peptides.** (A) The purified monomer, dimer, and trimer of recombinant 3xK-C100Flag were loaded on a SDS-PAGE gel and identified from the gel stained by Coomassie blue. The size of the monomer was at ~12 kDa (black arrow), the dimer was at ~24 kDa (grey arrow), and the trimer was at ~36 kDa (open arrow). (B–C) Western blot of the purified monomer, dimer, and trimer 3xK-C100Flag substrates before/after IVA did not show significant changes in relative amounts of the various multimers. (D) Aβ ELISAs showed that Aβ production measured from 3xK-C100Flag dimer substrate is significantly reduced compared to that from 3xK-C100Flag monomer, but that there is no evidence for major shifts in Aβ ratios (E). Aβ profiles generated from IP/MS of the media show that for 3xK-C100Flag there is increased relative production of longer Aβ isoforms compared to WT substrate (see Figure 2). Molecular mass (m/z) of monomeric 3xK-C100Flag for Aβ40 is 4588.43 (calculated m/z: 4589.27), for Aβ42 is 4773.07 (calculated m/z: 4773.51), and for Aβ45 is 5084.52 (calculated m/z: 5086.90). 3xK-C100Flag dimer and trimer showed decreased Aβ levels compared to the monomer. Molecular mass of dimeric 3xK-C100Flag for Aβ40 is 4587.48 (calculated m/z: 4589.27) and for Aβ42 is 4769.235 (calculated m/z: 4773.51). (F) AICD profiles show that C49-99 and C50-99 are the dominant peaks for 3xK-C100Flag monomer and that this profile is similar to that observed for WT substrate. Molecular mass (m/z) of monomeric 3xK-C100Flag for AICD50-99 is 6915.460 (calculated m/z: 6905.66), for AICD49-99 is 7027.141 (calculated m/z: 7018.82). AICD production from 3xK-C100Flag dimer and trimer is markedly decreased in comparison to monomer. This experiment was performed twice with duplicates. Results were analyzed by two-way analysis of variance (ANOVA) followed by bonferroni post hoc testing (\*\*\*\* $p < 0.0001$ ). doi:10.1371/journal.pone.0111553.g003

effects on  $\gamma$ -secretase processivity. Indeed, we did not observe increased multimerization of the recombinant 3xK-C100 FLAG substrate compared to WT substrate; both are highly aggregation prone supporting the assertion that the dimerization observed in the 3xK-APP isolated from cells is due to alterations in interactions of the TMD and lipids bilayer.

It is now clear that there are multiple different classes of GSMs and that different classes of GSMs may have different primary binding sites within the  $\gamma$ -secretase complex [53]. The current studies are most directly relevant to NSAID-based GSMs that can bind the tandem GXXXG motif in APP and alter processivity and dimerization [28,29] in what appears to be an independent fashion. In contrast, a mechanism of GSM action through primary binding to APP [28,29] would be difficult to reconcile with second generation GSMs that have been shown to bind PSEN or PEN-2 [45,47,49,54,55]. More generally, given the ample evidence for influence for substrate dependent effects of both acidic and non-acidic GSMs, we believe that it is over simplistic to view GSM mechanism of action solely based on determination of primary binding site [8,9,28,29,56]. It is clear that GSMs influence  $\gamma$ -secretase processivity in a complex way that involves both interactions of substrate and enzyme [9]. In conclusion, we found

that decreased  $\gamma$ -secretase processivity is related to intrinsic properties of the substrate rather than to the APP dimer induced by 3xK-APP mutation. Although reports from one group claim that dimeric substrates lead to decrease in  $\gamma$ -secretase processivity [26,28], the weight of published evidence suggests that this is not the case [31,32,34,57]. Our data offer both a positive example (mutant monomer is efficiently cleaved and shifts processivity) and reinforce the negative example (dimer/trimer are not cleaved or are cleaved very inefficiently). Collectively, these data suggest that APP dimer formation and  $\gamma$ -secretase processivity are dissociable; thus, they have important implications for design and screening of GSMs as therapeutic agents for AD.

## Supporting Information

**File S1 Figures S1 and S2. Figure S1. The CTFβ of WT- and 3xK-APP stably expressed into CHO cells.** The Western blot analysis shows the CTFβ expression in CHO cells probed with 6E10 and 82E1 antibodies. CTFβ bands from the 3xK-APP show lower expression and migrated slower than the WT-APP.  $\alpha$ -Tubulin and  $\beta$ -actin are provided as loading controls. **Figure S2. Purified recombinant WT-C100Flag and 3xK-**

**C100Flag form SDS-stable multimers analyzed by Western blot.** WT-C100Flag substrate and 3xK-C100Flag substrate were loaded on SDS-PAGE gels. The formation of (A) WT-C100Flag and (B) 3xK-C100Flag multimers was shown by Western blot analysis using 6E10 antibody that probes CTF $\beta$  following SDS-PAGE. Monomer (black), dimer (grey), and trimer (white) were indicated with arrows. (DOCX)

## References

- Glenner GG, Wong CW (1984) Alzheimer's disease and Down's syndrome: Sharing of a unique cerebrovascular amyloid fibril protein. *Biochem Biophys Res Commun* 122: 1131–1135.
- Wong CW, Quaranta V, Glenner GG (1985) Neuritic plaques and cerebrovascular amyloid in Alzheimer disease are antigenically related. *Proc Natl Acad Sci U S A* 82: 8729–8732.
- Masters CL, Simms G, Weinman NA, Multhaup G, McDonald BL, et al. (1985) Amyloid plaque core protein in Alzheimer disease and Down syndrome. *Proc Natl Acad Sci U S A* 82: 4245–4249.
- Seubert P, Oltschendorf T, Lee MG, Barbour R, Blomquist C, et al. (1993) Secretion of beta-amyloid precursor protein cleaved at the amino terminus of the beta-amyloid peptide. *Nature* 361: 260–263.
- Golde TE, Eckman CB, Younkin SG (2000) Biochemical detection of A $\beta$  isoforms: implications for pathogenesis, diagnosis, and treatment of Alzheimer's disease. *Biochim Biophys Acta* 1502: 172–187.
- Murphy MP, Hickman LJ, Eckman CB, Uljon SN, Wang R, et al. (1999)  $\gamma$ -Secretase, Evidence for Multiple Proteolytic Activities and Influence of Membrane Positioning of Substrate on Generation of Amyloid  $\beta$  Peptides of Varying Length. *J Biol Chem* 274: 11914–11923.
- Wang R, Sweeney D, Gandy SE, Sisodia SS (1996) The Profile of Soluble Amyloid  $\beta$  Protein in Cultured Cell Media: DETECTION AND QUANTIFICATION OF AMYLOID  $\beta$  PROTEIN AND VARIANTS BY IMMUNOPRECIPITATION-MASS SPECTROMETRY. *J Biol Chem* 271: 31894–31902.
- Kukar TL, Ladd TB, Robertson P, Pintchovski SA, Moore B, et al. (2011) Lysine 624 of the Amyloid Precursor Protein (APP) Is a Critical Determinant of Amyloid  $\beta$  Peptide Length. *J Biol Chem* 286: 39804–39812.
- Jung JI, Ran Y, Cruz PE, Rosario AM, Ladd TB, et al. (2014) Complex Relationships between Substrate Sequence and Sensitivity to Alterations in  $\gamma$ -Secretase Processivity Induced by  $\gamma$ -Secretase Modulators. *Biochemistry* 53: 1947–1957.
- Ran Y, Cruz PE, Ladd TB, Fauq AH, Jung JI, et al. (2014)  $\gamma$ -Secretase Processing and Effects of  $\gamma$ -Secretase Inhibitors and Modulators on Long A $\beta$  Peptides in Cells. *J Biol Chem* 289: 3276–3287.
- Younkin S (1998) The role of A beta 42 in Alzheimer's disease. *J Physiol Paris* 92: 289–292.
- Borchelt DR, Thinakaran G, Eckman CB, Lee MK, Davenport F, et al. (1996) Familial Alzheimer's Disease-Linked Presenilin 1 Variants Elevate A $\beta$ 1–42/1–40 Ratio In Vitro and In Vivo. *Neuron* 17: 1005–1013.
- Duff K, Eckman C, Zehr C, Yu X, Prada C-M, et al. (1996) Increased amyloid- $\beta$ 42(43) in brains of mice expressing mutant presenilin 1. *Nature* 383: 710–713.
- Scheuner D (1996) Secreted amyloid  $\beta$ -protein similar to that in the senile plaques of Alzheimer's disease is increased in vivo by the presenilin 1 and 2 and APP mutations linked to familial Alzheimer's disease. *Nat Med* 2: 864–870.
- Murayama O, Tomita T, Nihonmatsu N, Murayama M, Sun X, et al. (1999) Enhancement of amyloid  $\beta$  42 secretion by 28 different presenilin 1 mutations of familial Alzheimer's disease. *Neurosci Lett* 265: 61–63.
- Gravina SA, Ho L, Eckman CB, Long KE, Otvos L, et al. (1995) Amyloid  $\beta$  Protein (A $\beta$ ) in Alzheimer's Disease Brain. *J Biol Chem* 270: 7013–7016.
- Iwatsubo T, Odaka A, Suzuki N, Mizusawa H, Nukina N, et al. (1994) Visualization of A $\beta$ 42(43) and A $\beta$ 40 in senile plaques with end-specific A $\beta$  monoclonals: Evidence that an initially deposited species is A $\beta$ 42(43). *Neuron* 13: 45–53.
- Moore BD, Chakrabarty P, Levites Y, Kukar TL, Baine A-M, et al. (2012) Overlapping profiles of Abeta peptides in the Alzheimer's disease and pathological aging brains. *Alzheimers Res Ther* 4: 18.
- Jarrett JT, Lansbury Jr PT (1993) Seeding "one-dimensional crystallization" of amyloid: A pathogenic mechanism in Alzheimer's disease and scrapie? *Cell* 73: 1055–1058.
- Jarrett JT, Berger EP, Lansbury PT (1993) The carboxy terminus of the beta-amyloid protein is critical for the seeding of amyloid formation: Implications for the pathogenesis of Alzheimer's disease. *Biochemistry* 32: 4693–4697.
- McGowan E, Pickford F, Kim J, Onstead L, Eriksen J, et al. (2005) Abeta42 is essential for parenchymal and vascular amyloid deposition in mice. *Neuron* 47: 191–199.
- Saito T, Suemoto T, Brouwers N, Slegers K, Funamoto S, et al. (2011) Potent amyloidogenicity and pathogenicity of Abeta43. *Nat Neurosci* 14: 1023–1032.

## Acknowledgments

We thank Patricia Joy for critical reading of this manuscript.

## Author Contributions

Conceived and designed the experiments: JJJ TEG YR. Performed the experiments: JJJ SP PEC YK YR. Analyzed the data: TBL EHK KMF TEG YR. Contributed to the writing of the manuscript: JJJ EHK TEG YR.

- Conicella AE, Fawzi NL (2014) The C-terminal threonine of A $\beta$ 43 nucleates toxic aggregation via structural and dynamical changes in monomers and protofibrils. *Biochemistry*: Epub ahead of print.
- Takami M, Nagashima Y, Sano Y, Ishihara S, Morishima-Kawashima M, et al. (2009)  $\gamma$ -Secretase: Successive Tripeptide and Tetrapeptide Release from the Transmembrane Domain of  $\beta$ -Carboxyl Terminal Fragment. *J Neurosci* 29: 13042–13052.
- Matsumura N, Takami M, Okochi M, Wada-Kakuda S, Fujiwara H, et al. (2013)  $\gamma$ -Secretase associated with lipid rafts: multiple interactive pathways in the stepwise processing of  $\beta$ -carboxyl terminal fragment. *J Biol Chem* 289: 5109–5121.
- Munter LM, Voigt P, Harmeier A, Kaden D, Gottschalk KE, et al. (2007) GxxxG motifs within the amyloid precursor protein transmembrane sequence are critical for the etiology of A $\beta$ 42. *EMBO J* 26: 1702–1712.
- Scheuermann S, Hamsch B, Hesse L, Stumm J, Schmidt C, et al. (2001) Homodimerization of amyloid precursor protein and its implication in the amyloidogenic pathway of Alzheimer's disease. *J Biol Chem* 276: 33923–33929.
- Richter L, Munter L-M, Ness J, Hildebrand PW, Dasari M, et al. (2010) Amyloid beta 42 peptide (A $\beta$ 42)-lowering compounds directly bind to A $\beta$  and interfere with amyloid precursor protein (APP) transmembrane dimerization. *Proc Natl Acad Sci USA* 107: 14597–14602.
- Kukar TL, Ladd TB, Bann MA, Fraering PC, Narlawar R, et al. (2008) Substrate-targeting  $\gamma$ -secretase modulators. *Nature* 453: 925–929.
- So PP, Zeldich E, Seyb KI, Huang MM, Concannon JB, et al. (2012) Lowering of amyloid beta peptide production with a small molecule inhibitor of amyloid- $\beta$  precursor protein dimerization. *American journal of neurodegenerative disease* 1: 75–87.
- Eggert S, Midthune B, Cottrell B, Koo EH (2009) Induced Dimerization of the Amyloid Precursor Protein Leads to Decreased Amyloid- $\beta$  Protein Production. *J Biol Chem* 284: 28943–28952.
- Vooijs M, Schroeter EH, Pan Y, Blandford M, Kopan R (2004) Ectodomain Shedding and Intramembrane Cleavage of Mammalian Notch Proteins Are Not Regulated through Oligomerization. *J Biol Chem* 279: 50864–50873.
- Kienlen-Campard P, Tasiaux B, Van Hees J, Li M, Huysseune S, et al. (2008) Amyloidogenic Processing but Not Amyloid Precursor Protein (APP) Intracellular C-terminal Domain Production Requires a Precisely Oriented APP Dimer Assembled by Transmembrane GXXXG Motifs. *J Biol Chem* 283: 7733–7744.
- Struhl G, Adachi A (2000) Requirements for Presenilin-Dependent Cleavage of Notch and Other Transmembrane Proteins. *Mol Cell* 6: 625–636.
- Kimberly WT, Esler WP, Ye W, Ostaszewski BL, Gao J, et al. (2003) Notch and the Amyloid Precursor Protein Are Cleaved by Similar  $\gamma$ -Secretase(s). *Biochemistry* 42: 137–144.
- Alcaraz C, De Diego M, Pastor MJ, Escibano JM (1990) Comparison of a Radioimmunoprecipitation Assay to Immunoblotting and ELISA for Detection of Antibody to African Swine Fever Virus. *J Vet Diagn Invest* 2: 191–196.
- Kukar T, Murphy MP, Eriksen JL, Sagi SA, Weggen S, et al. (2005) Diverse compounds mimic Alzheimer disease-causing mutations by augmenting A $\beta$ 42 production. *Nat Med* 11: 545–550.
- Wang R, Sweeney D, Gandy S, Sisodia S (1996) The profile of soluble amyloid beta protein in cultured cell media. Detection and quantification of amyloid beta protein and variants by immunoprecipitation-mass spectrometry. *J Biol Chem* 271: 31894–31902.
- Murphy MP, Uljon SN, Fraser PE, Fauq A, Lookingbill HA, et al. (2000) Presenilin 1 Regulates Pharmacologically Distinct  $\gamma$ -Secretase Activities: IMPLICATIONS FOR THE ROLE OF PRESENILIN IN  $\gamma$ -SECRETASE CLEAVAGE. *J Biol Chem* 275: 26277–26284.
- Levites Y, Das P, Price RW, Rochette MJ, Kostura LA, et al. (2006) Anti-A $\beta$ 42- and anti-A $\beta$ 40-specific mAbs attenuate amyloid deposition in an Alzheimer disease mouse model. *J Clin Invest* 116: 193–201.
- Esler WP, Kimberly WT, Ostaszewski BL, Ye W, Diehl TS, et al. (2002) Activity-dependent isolation of the presenilin- $\gamma$ -secretase complex reveals nicastrin and a  $\gamma$  substrate. *Proc Natl Acad Sci USA* 99: 2720–2725.
- Fraering PC, Ye W, LaVoie MJ, Ostaszewski BL, Selkoe DJ, et al. (2005)  $\gamma$ -Secretase Substrate Selectivity Can Be Modulated Directly via Interaction with a Nucleotide-binding Site. *J Biol Chem* 280: 41987–41996.
- Watt A, Perez K, Rembach A, Sherratt N, Hung L, et al. (2013) Oligomers, fact or artefact? SDS-PAGE induces dimerization of  $\beta$ -amyloid in human brain samples. *Acta Neuropathologica* 125: 549–564.

44. Botev A, Munter L-M, Wenzel R, Richter L, Althoff V, et al. (2010) The Amyloid Precursor Protein C-Terminal Fragment C100 Occurs in Monomeric and Dimeric Stable Conformations and Binds  $\gamma$ -Secretase Modulators. *Biochemistry* 50: 828–835.
45. Pozdnyakov N, Murrey HE, Crump CJ, Pettersson M, Ballard TE, et al. (2013)  $\gamma$ -Secretase modulator (GSM) photoaffinity probes reveal distinct allosteric binding sites on presenilin. *J Biol Chem* 288: 9710–9720.
46. Ohki Y, Higo T, Uemura K, Shimada N, Osawa S, et al. (2011) Phenylpiperidine-type gamma-secretase modulators target the transmembrane domain 1 of presenilin 1. *EMBO J* 30: 4815–4824.
47. Jumpertz T, Rennhack A, Ness J, Baches S, Pietrzik CU, et al. (2012) Presenilin is the molecular target of acidic gamma-secretase modulators in living cells. *PLoS ONE* 7: e30484.
48. Ebke A, Luebbbers T, Fukumori A, Shirovani K, Haass C, et al. (2011) Novel gamma-secretase enzyme modulators directly target presenilin protein. *J Biol Chem* 286: 37181–37186.
49. Kounnas MZ, Danks AM, Cheng S, Tyree C, Ackerman E, et al. (2010) Modulation of  $\gamma$ -Secretase Reduces  $\beta$ -Amyloid Deposition in a Transgenic Mouse Model of Alzheimer's Disease. *Neuron* 67: 769–780.
50. Wang H, Barreyro L, Provasi D, Djemil I, Torres-Arancivia C, et al. (2011) Molecular Determinants and Thermodynamics of the Amyloid Precursor Protein Transmembrane Domain Implicated in Alzheimer's Disease. *J Mol Biol* 408: 879–895.
51. Strandberg E, Killian JA (2003) Snorkeling of lysine side chains in transmembrane helices: how easy can it get? *FEBS Lett* 544: 69–73.
52. Song Y, Hustedt EJ, Brandon S, Sanders CR (2013) Competition Between Homodimerization and Cholesterol Binding to the C99 Domain of the Amyloid Precursor Protein. *Biochemistry* 52: 5051–5064.
53. Golde TE, Koo EH, Felsenstein KM, Osborne BA, Miele L (2013)  $\gamma$ -Secretase inhibitors and modulators. *Biochimica et Biophysica Acta (BBA) - Biomembranes* 1828: 2898–2907.
54. Ohki Y, Higo T, Uemura K, Shimada N, Osawa S, et al. (2011) Phenylpiperidine-type [gamma]-secretase modulators target the transmembrane domain 1 of presenilin 1. *EMBO J* 30: 4815–4824.
55. Ebke A, Luebbbers T, Fukumori A, Shirovani K, Haass C, et al. (2011) Novel  $\gamma$ -Secretase Enzyme Modulators Directly Target Presenilin Protein. *J Biol Chem* 286: 37181–37186.
56. Sagi SA, Lessard CB, Winden KD, Maruyama H, Koo JC, et al. (2011) Substrate Sequence Influences  $\gamma$ -Secretase Modulator Activity, Role of the Transmembrane Domain of the Amyloid Precursor Protein. *J Biol Chem* 286: 39794–39803.
57. Kienlen-Campard P, Tasiaux B, Van Hees J, Li M, Huysseune S, et al. (2008) Amyloidogenic Processing but Not Amyloid Precursor Protein (APP) Intracellular C-terminal Domain Production Requires a Precisely Oriented APP Dimer Assembled by Transmembrane GXXXG Motifs. *Journal of Biological Chemistry* 283: 7733–7744.